Shielding of resonant magnetic perturbations in the long mean-free path regime

F. L. Waelbroeck

Institute for Fusion Studies, University of Texas at Austin

(Dated: June 28, 2003)

Abstract

The effect of diamagnetic drifts and of long electron mean free path on the shielding of resonant magnetic perturbations by plasma rotation is investigated. The nature of the force exerted on a moving plasma by a resonant perturbation is qualitatively altered by both drift and long mean-free-path effects. The force is found to have three minima, each of which is a possible locus for discontinuous transitions in plasma velocity. Between these minima are two points where the force exerted by the perturbation is resonant. These points describe locked states where shielding is ineffective and a magnetic island will grow. They correspond to rotation velocities such that either the electrons or the ions are at rest in the frame of the perturbation. The ion root, however, is unstable.

PACS numbers: 52.30.Ex, 52.55.Tn, 52.35.Vd,52.40.Fd

I. INTRODUCTION

The resonant response of a magnetized plasma in resonant layers where the wavefront is parallel to the magnetic field is of interest in many contexts. In axisymmetric systems, it influences the dynamics of wall modes,[1, 2, 3, 4] the interaction between the various internal modes,[5, 6] and the effect of externally imposed perturbations such as feedback corrections[7, 8, 9] and error fields.[10, 11, 12, 13, 14, 15, 16, 17, 18, 19, 20, 21, 22, 23] In helical systems a favorable magnetic well has been shown to lead to the healing of magnetic islands.[24]

In a static plasma resonant perturbations give rise, through magnetic reconnection, to islands of widths proportional to the square root of the transverse displacement at a large distance from the island.[15] Magnetic reconnection is strongly inhibited, however, in the presence of even modest levels of plasma motion.[10, 17, 21] The primary effect of the perturbations is then to exert a braking force on the plasma. When the perturbation exceeds a threshold amplitude, the plasma is abruptly stopped and reconnection proceeds to saturation.[17, 18] The transition between the kinematically shielded and the reconnecting states is known as mode penetration.[17]

The plasma braking and mode penetration phenomena are well characterized experimentally.[11, 13, 18, 25] Two manifestations of these phenomena have received particular attention due to their importance for tokamak operation. The first is the penetration of coil-alignment errors, giving rise to the so-called low density locked modes (LDLM).[18] The second is the seeding of magnetic islands during magnetic activity such as sawtooth, fishbone and the edge localized mode (ELM).[26] It has also been shown experimentally that the mode-penetration threshold becomes vanishingly small when the plasma is heated towards its ideal stability limit.[12] More recently, Garofalo et al. have shown that error fields are amplified when the plasma pressure rises above the value where stabilization by a conducting wall is required. The amplification of the error fields causes the onset of plasma deceleration and leads to disruptions.[2, 3]

Although present and future fusion experiments operate in the long mean-free-path regime, most of the existing theoretical results, both analytic[5, 6, 16, 17, 19, 21, 22, 23] and numerical,[14, 15, 20, 27] are based on low beta Magnetohydrodynamics (MHD) in slab geometry. An exception is the early paper by Fitzpatrick and Hender,[10] which dis-

cussed kinematic shielding in the presence of diamagnetic drifts. This paper assumed a collisional plasma response, however, and did not consider rotation braking or mode penetration. While the existing collisional theory is reasonably successful in accounting for the experimental observations,[11] it cannot be extrapolated with confidence to burning plasma experiments.

The purpose of the present paper is to investigate the effect of long mean free path on rotation braking and on the mode penetration threshold. In order to simplify the analysis, we use a fluid model with cold ions, but retain drift terms and, crucially, the electron pressure term in Ohm's law. The existing theory for tearing modes shows that this model correctly describes essentially all the features of long mean-free path physics found in more detailed kinetic descriptions.[28, 29, 30]

The paper is organized as follows. We begin in Sec. II by describing the model used in our analysis. In Sec. III we describe analytic solutions in various asymptotic regimes. We compare these analytic solutions to numerical solutions in Sec. IV before concluding in section V.

II. FORMULATION

A. Description of the plasma

We consider a periodic sheared slab geometry with a magnetic field given by

$$\mathbf{B} = B_0\hat{\mathbf{z}} - \boldsymbol{\nabla}\psi(x,y) \times \hat{\mathbf{z}}, \tag{1}$$

where B_0 is a constant magnetic field pointing in the symmetry direction $\hat{\mathbf{z}} = \boldsymbol{\nabla} z$, and where the azimuthal magnetic flux ψ is related to the longitudinal vector potential A_z by $\psi = -A_z$. The reference state is chosen such that $\psi_0 = -B_0 x^2/2L_s$, where L_s is the magnetic shear length. We consider a perturbed azimuthal flux of the form $\psi = \psi_0 + \tilde{\psi}\cos k_y y$, where y is the azimuthal coordinate. At the surface $x = 0$, the phase of the perturbation is constant along the magnetic field so that the electrostatic shielding of the inductive field perturbation is disabled. This leads to a resonant current response.

The above sheared-slab geometry can be considered to model a large aspect-ratio tokamak by making the correspondence $x = r - r_s$, where r is the minor radius and $r = r_s$ is the radius of the resonant surface, and $k_y y = m\theta - n\zeta$ where θ and ζ are the poloidal and

toroidal angles, and m and n are the poloidal and toroidal mode numbers. The shear-length is related to the tokamak parameters by $L_s = Rq/s$, where R is the major radius, q is the safety factor, and $s = (r/q)dq/dr$ is the magnetic shear.

The long mean free path regime that is the object of this paper is defined by $k_\parallel^2 v_{te}^2 \gg \omega\nu_{ei}$, where $k_\parallel = \mathbf{k}\cdot\mathbf{B}/B$ is the parallel component of the wavevector, v_{te} is the thermal velocity of the electron, and ν_{ei} is the electron-ion collision frequency. [28, 31] The principal features of the dispersion relation for tearing modes in this long mean free path regime are known to be correctly predicted by the two-fluid, drift-MHD model.[31, 32, 33] To simplify the analysis, we consider here only the cold ion model ($T_i = 0$). Furthermore, we will restrict consideration to weak shear systems for which $k_\parallel c_s \ll \omega_*$, where $k_\parallel$ is the parallel component of the wavevector and c_s is the sound speed. For such systems we may neglect the ion parallel motion. We denote the convective time derivative along the $\mathbf{E}\times\mathbf{B}$ flow by D/Dt,

$$\frac{D}{Dt} = \frac{\partial}{\partial t} + \mathbf{v}_E\cdot\boldsymbol{\nabla},$$

where $\mathbf{v}_E$, the electric drift velocity, is related to the electrostatic potential ϕ by $\mathbf{v}_E = (c/B_0)\hat{\mathbf{z}}\times\boldsymbol{\nabla}\phi$. Note that since $T_i = 0$, $\mathbf{v}_E$ is approximately equal to the ion fluid velocity. The electron continuity equation is then

$$\frac{Dn}{Dt} = \frac{1}{e}\nabla_\parallel J_\parallel, \tag{2}$$

where n is the density (equal for ions and electrons by quasi-neutrality), e is the electron charge, $J = (c/4\pi)\nabla^2\psi$ is the parallel current, $\nabla_\parallel = (\mathbf{B}/B)\cdot\boldsymbol{\nabla}$ and $\boldsymbol{\nabla}_\perp$ represent the gradients respectively along and transverse to the magnetic field. The quasi-neutrality condition requires $\nabla\cdot\mathbf{J} = 0$, or

$$\nabla_\parallel J_\parallel = \frac{c^2}{4\pi v_A^2}\left[\frac{DU}{Dt} - \mu\boldsymbol{\nabla}_\perp^2 U\right], \tag{3}$$

where $U = \boldsymbol{\nabla}_\perp^2\phi$ is proportional to the vorticity, and μ is the viscosity. Eq. (3) can be viewed alternatively as a vorticity or a local force-balance equation. Lastly, we use Ohm's law in the form

$$E_\parallel + \frac{\nabla_\parallel p}{ne} = \frac{J_\parallel}{\sigma_\parallel}, \tag{4}$$

where $E_\parallel = (1/c)\partial\psi/\partial t - \nabla_\parallel\phi$ is the parallel electric field and p is the plasma pressure.

B. Plasma Response to external perturbations

For large Lundquist numbers one may separate the response of the plasma into a diffuse and a resonant response. The diffuse response is caused by the currents excited throughout the bulk of the plasma where the phase of the wave varies along field lines. The effect of the diffuse plasma currents is generally to amplify the perturbation by a factor of $\mathcal{A}$ compared to its vacuum value. The resonant current response, by contrast, is of much larger amplitude but is confined to a thin layer around the resonant surface.

The quantities of interest for comparison with experiment are the threshold amplitude for field penetration and the braking force. These quantities are determined by the amplitude of the transverse field perturbation at the resonant surface. We summarize here for future reference the relevant formulae.[17] The transverse field perturbation is proportional to the amplitude of the flux perturbation, given by

$$\Psi = \frac{\mathcal{A}^2 |\Psi_{vac}|}{|1 + \Delta(\omega)/(-\Delta')|}, \tag{5}$$

where $\Delta(\omega)$ and Δ' describe respectively the response of the layer and the stability parameter for the tearing mode.[34] We will give a precise definition of Δ in Eq. (12) below. In the absence of an imposed perturbation, the only solutions are eigenmodes satisfying $\Delta(\omega) = \Delta'$. The phase difference between the current and field perturbation is

$$\varphi = \tan^{-1}\left[\frac{\Im(\Delta(\omega)/(-\Delta'))}{1 + \Re(\Delta/(-\Delta'))}\right] \tag{6}$$

The force per unit area acting on the resonant layer is given in terms of these two quantities by

$$F = \frac{k\Delta'}{8\pi}\mathcal{A}^2 \Psi \Psi_{vac} \sin\varphi. \tag{7}$$

In the present paper we will only consider the calculation of the layer impedance $\Delta(\omega)$. The amplification factor $\mathcal{A}$ and stability parameter Δ' depend on details of the equilibrium. Their calculation is best carried out with finite element codes working from equilibrium reconstructions.

C. Layer equations

We wish to find solutions of (2)-(4) that are independent of time in a frame where the perturbation is at rest (e.g. the lab frame for an error field). We thus set $\partial/\partial t = 0$ and

define the plasma rotation frequency in the frame of the perturbation as $\omega = k_y V_E$. Note that if the perturbation is caused by a propagating mode, the frequency ω defined here is the negative of the mode frequency in the frame where $E_x = 0$.

Recalling that the force is determined quasi-linearly from the properties of the linear solution,[17] we linearize Equations (2)-(4) and cast them in standard form by eliminating the density with the help of the continuity equation. We introduce the normalized coordinate $X = x/\delta$ describing the distance across the resonant surface, where $\delta = (c^2 L_s/4\pi\sigma_\parallel k_y v_A)^{1/3}$ is the the characteristic width obtained by equating the rate of resistive diffusion with the shear-Alfvén frequency. We normalize the remaining variables according to $\hat{\Delta} = \Delta\delta$, $\Xi = \tilde{\phi}/\delta\phi_0'$, $\Psi = \tilde{\psi}/\delta^2\psi_0'' = L_s\tilde{\psi}/\delta^2 B_0$, and $Q = k_y v_E/\gamma$ where $\gamma = k_y V_A \delta/L_s$ is the characteristic growth rate for the resistive interchange and kink-tearing instabilities, and $\tilde{\phi}$, $\tilde{\psi}$ represent the perturbed quantities.

The system to be solved is then formed by Ohm's law and the vorticity equation,

$$X\Psi'' = Q^2\Xi'' - iPQ\Xi'''', \tag{8}$$

$$\Psi'' = -i\Sigma(X)(Q - Q_*)(\Psi - X\Xi), \tag{9}$$

where the primes denote differentiation with respect to X, and $\Sigma(X)$ is the conductivity. For the cold ion fluid model used here,

$$\Sigma = \frac{1}{1 + iR^2X^2/Q}, \tag{10}$$

where $R = \rho_s/\delta$.

Eqs. (8)-(9) differ from the corresponding equations for the magnetohydrodynamic (MHD) model in two ways. First, the frequency appearing in Ohm's law is shifted by the electron drift frequency Q_*. Second, the conductivity Σ, which is unity in MHD with the normalization used here, becomes spatially dependent in the long mean-free path regime. Specifically, the conductivity peaks in a channel of width $X_\sigma = \sqrt{|Q|}/R$ centered on the resonant surface $X = 0$.

We note that Eqs. (8)-(9) conserve parity and admit the trivial solution $\Psi = X$, $\Xi = 1$. We may thus restrict consideration to solutions for which Ψ is even in X. It is convenient to introduce the quantity

$$\Gamma(X) = X\Psi' - \Psi, \tag{11}$$

representing the intercept between the ordinate and the tangent to the graph of $\Psi(X)$ at X. The parameter $\hat{\Delta}$ that serves to match the layer solutions to the external perturbation is defined in terms of Γ by

$$\hat{\Delta}(Q) = -2 \lim_{X\to\infty} \frac{\Psi'(X)}{\Gamma(X)} = -2\frac{\Psi'_\infty}{\Gamma_\infty}. \tag{12}$$

We conclude our presentation of the governing equations with a brief review of the known solutions of Eqs. (8)-(9). In the short mean-free-path limit $R \to 0$, Coppi et al.[35] have given a complete analytic solution for the inviscid MHD limit $P = 0$ and $Q_* = 0$. Ara et al. have discussed the generalization of that solution to the case $|Q_*| > 0$.[36] In the viscous case, an exhaustive set of solutions describing all four possible orderings has been described by Fitzpatrick.[37]

In the long mean-free-path regime, by contrast, Eqs. (8)-(9) have only been studied in the context of finding the growth rates for resistive eigenmodes. In this context the inviscid limit has been described by Drake and Lee for ordinary tearing modes,[28] and by Drake[29] and Mahajan et al.[30] for the kink-tearing mode. In the present paper we extend the work of Drake to include viscosity, and apply the results to the description of rotation braking and mode penetration by resonant perturbation.

III. ANALYTIC SOLUTIONS

In this section we describe solutions to Eqs (8)-(9) in various asymptotic regimes, and map the boundaries between these regimes in parameter space. The various regimes are characterized by the relative dimension of three characteristic widths. The first of these is the half-distance between Alfvén resonances, $X_A = Q$. The second is the width $X_\sigma = \sqrt{Q}/R$ of the conductivity channel. The third is the width of the vorticity layer. This third width depends on the relative importance of viscosity compared to polarization effects, and will be calculated below.

We first consider the limit of low frequency. In this limit, the width δ_σ of the conductivity channel approaches zero. When δ_σ is smaller than the characteristic width for electrostatic screening of the perturbation, we may neglect the $X\Xi$ term in Eq. (9). Using the constant-Ψ approximation, we find that

$$\Psi'' = \frac{-i(Q - Q_*)\Psi(0)}{1 + iX^2R^2/Q}. \tag{13}$$

We recover the result familiar from previous long mean-free-path tearing mode studies that the current is confined to a narrow channel of width X_σ.[28, 29, 30, 31] The validity of using the constant-Ψ approximation in the conductivity channel requires that $X_\sigma \hat{\Delta}(Q) \ll 1$, or $Q(Q-Q_*) \ll R^2$. Integrating Eq. (13) yields

$$2\Psi'_\infty = \pi \exp(-3i\pi/4)(Q-Q_*)\frac{\sqrt{Q}}{R}\Psi(0) \tag{14}$$

In order to evaluate the matching parameter $\Delta(Q)$ we must express $\Psi(0)$ in terms of Γ_∞ and Ψ'_∞. We note that the conductivity channel is embedded in a broader layer defined by the resonant response of the ions. While the total perturbed current flowing outside of the conductivity channel is small compared to that flowing within it, the current outside the channel may still affect the matching parameter through Γ_∞. To see this, note that Γ is related to the current by

$$\Psi(0) = -\Gamma(0) = -\Gamma_\infty + \int_0^\infty dX\, X\Psi''. \tag{15}$$

The integral of the current in the right hand side is weighted by the distance from the resonant surface, so that the current outside the channel may contribute to Γ_∞ even though it is too small to change Ψ'_∞ in any appreciable way. When this is the case we may make the approximation $\Psi \simeq \Psi(0) + \Psi'_\infty X$ to calculate the perturbed fields outside the channel. We will see however that $\Psi(0) \ll \Psi'_\infty X$ over most of the resonant layer, so that we may make the further approximation $\Psi \simeq \Psi'_\infty X$. We will refer to this approximation, due to Drake,[29] as the constant-Ψ' approximation. A limitation of the constant-Ψ' approximation is that it is invalid in the transition region between the current channel and the outer resonant layer, so that it cannot be used to demonstrate the smooth matching of the solutions in these two regions. This is a subject for concern since the contribution of the current channel to $\Gamma(X)$ is unbounded. This subject is addressed in the Appendix, where a solution that retains $\Psi(0)$ is obtained and shown to match smoothly to the channel solution.

To calculate the perturbed quantities outside the current channel, we eliminate the current from (8)-(9). This yields the equation for Ξ,

$$M\left(\frac{d}{dX}\right)\Xi(X) = -(Q-Q_*)\frac{\Psi(X)}{X}, \tag{16}$$

where M is the quartic polynomial defined by

$$M(\lambda) = -iR^2P\lambda^4 + R^2Q\lambda^2 - (Q-Q_*), \tag{17}$$

We separate the displacement into $\Xi = \Xi_\ell + \Xi_t$, where

$$M(d/dX)\,\Xi_\ell(X) \;=\; -(Q-Q_*)\Psi'_\infty, \tag{18}$$

$$M(d/dX)\,\Xi_t(X) \;=\; -(Q-Q_*)\Psi(0)\,X^{-1}. \tag{19}$$

One may interpret these parts by thinking of Ξ_ℓ as driven by the longitudinal magnetic field perturbation, proportional to Ψ'_∞, and of Ξ_t as driven by the transverse magnetic field perturbation, proportional to $\Psi(0)$. The transverse part is only important in a transition region between the outer layer and the current channel, and does not contribute to the layer response parameter $\hat{\Delta}(Q)$. It is calculated in appendix A.

The solution for the longitudinal response is

$$\Xi_\ell(X) = \Psi'_\infty[\Theta(X) - \alpha_+ \exp(\lambda_+ x) - \alpha_- \exp(\lambda_- X)], \tag{20}$$

where

$$\lambda_\pm^2 = -\frac{iQ}{2P}\left(1 \pm \sqrt{1 - \frac{4iP(Q-Q_*)}{Q^2R^2}}\right) \tag{21}$$

are the roots of $M(\lambda_\pm) = 0$. Continuity at the origin requires that

$$\alpha_\pm = \pm\frac{\lambda_\mp^2}{\lambda_-^2 - \lambda_+^2}. \tag{22}$$

The outer layer width is thus given by $w_{\rm out} = \{\min[\Re(\lambda_+), \Re(\lambda_-)]\}^{-1}$.

We next consider the first integral of Ohm's law,

$$\Gamma(X) = Q^2\Xi'(X) - iQP\Xi'''(X) + \Gamma_\infty. \tag{23}$$

We neglect Ξ_t and use $\Gamma(0) = -\Psi(0)$ to find

$$\Gamma_\infty + \Psi(0) = iQP\Xi'''_\ell(0) - Q^2\Xi'_\ell(0). \tag{24}$$

Using the solution for Ξ given in Eq. (20)-(22) to evaluate the right-hand side of (24) yields

$$\frac{1}{\Delta(Q)} = \frac{1}{\Delta_{\rm ch}} + \frac{1}{\Delta_{\rm out}}, \tag{25}$$

where

$$\Delta_{\rm ch} = \frac{2\Psi'_\infty}{\Psi(0)} = \pi e^{-3i\pi/4}(Q-Q_*)\frac{\sqrt{Q}}{R} \tag{26}$$

and

$$\Delta_{\rm out} = \frac{2R^2}{Q(Q-Q_*)}\,\frac{\lambda_-\lambda_+(\lambda_-^2 - \lambda_+^2)}{\lambda_-^3 - \lambda_+^3}. \tag{27}$$

Equations (25)-(27) form the principal analytic result of this paper. It is useful to consider their limiting forms to obtain simple scaling expression for the experimentally relevant quantities. We will use the results of the analysis of the limiting forms to construct a chart of the parameter space describing the three regimes that are governed by Eqs. (25)-(27), and will complete the chart with the inertial regime that governs the response at high frequency. Fig. 1 summarizes the various regimes and their boundaries as a function of Q and P.

A. Semi-collisional regime

In the limit of vanishing frequency, we find that the $\lambda_\pm$ remain finite, so that $\Delta_{\rm out}^{-1} \to 0$. It follows that the external layer does not contribute to the matching parameter:

$$\hat{\Delta}(Q) = \Delta_{\rm ch}(Q) = \pi \exp(i\pi/4) \frac{Q^{1/2}(Q - Q_*)}{R} \tag{28}$$

This is the semi-collisional regime of tearing mode theory. The boundaries of the semi-collisional regime correspond to $\Delta_{\rm ch} \simeq \Delta_{\rm out}$. Inspection of Eq. (21), however, reveals that $\Delta_{\rm out}$ takes different forms depending on the relative magnitude of the viscosity parameter P and $Q^2R^2/(Q - Q_*)$. We consider the low and high viscosity cases in turn.

B. Kinetic Alfvén Wave regime

In the inviscid limit, $P \ll Q^2R^2/(Q-Q_*)$, we may expand Eq. (21) to find $\lambda_- \simeq \sqrt{-iQ/P}$ and

$$\lambda_+ \simeq (\sqrt{1 - Q_*/Q})/R \left(1 + iP(Q - Q_*)/(Q^2R^2)\right),$$

where we have kept the small viscous correction term since it determines the real part of λ_+ in the frequency band $1 < Q_*/Q$. In this frequency band the lowest-order term in λ_+ is purely imaginary, indicating that the response of the plasma is spatially oscillatory. The outer layer width is

$$w_{\rm out} = \begin{cases} R/\sqrt{1 - Q_*/Q}, & Q_*/Q < 1 \\ QR^3/(|1 - Q_*/Q|^{3/2}P), & 1 < Q_*/Q. \end{cases} \tag{29}$$

Eq. (27) yields

$$\Delta_{\rm out} = \frac{2R}{Q^{3/2}(Q - Q_*)^{1/2}} \tag{30}$$

Comparing this to the contribution of the current channel given by Eq. (28), we see that for $Q^2(Q-Q_*)^{3/2} \gg R^2$, the contribution of the current channel is negligible and $\Delta \simeq \Delta_{\rm out}$. The constant-$\Psi'$ approximation also requires that $w_{\rm out} > Q$. The regime described by this ordering is similar to the ideal regime aside from the effect of ρ_s or R. For this reason we will refer to it as the Kinetic Alfvén Wave (KAW) regime.

C. Visco-inertial regime

In the viscous regime, $P \gg Q^2R^2/(Q-Q_*)$, the limiting form of the parameters in the outside layer are $\lambda_\pm^2 \simeq \pm\sqrt{i(Q-Q_*)/R^2P}$. The layer width is thus

$$w_{\rm out} = [R^2P/(Q-Q_*)]^{1/4}$$

and the matching parameter

$$\Delta_{\rm out} = \frac{2\sqrt{2}\,\epsilon\, e^{i\pi\epsilon/8}R^{3/2}}{Q(Q-Q_*)^{3/4}P^{1/4}}, \tag{31}$$

where $\epsilon = \mathrm{sign}(Q-Q_*)$. The contribution of the viscous layer dominates that from the current channel when $P \gg R^{10}/Q^6(Q-Q_*)^7$.

D. Inertial regime

Lastly, we review for completeness the solution in the high frequency limit, where the resonance separates into two Alfvén wave resonances at $X = \pm X_A = \pm Q$. Neglecting nonideal and drift effects, we find

$$\Xi'(X) = \frac{1}{X^2-Q^2} \tag{32}$$

Due to the first-order nature of the separated resonances, the precise nature of the non-ideal mechanism becomes unimportant since the resonances can be resolved by analytic continuation. The solution is thus independent of P and of R. It is indistinguishable from the solution for the short mean-free-path case. The matching parameter in this regime is

$$\hat{\Delta}(Q) = i\frac{\pi}{Q} \tag{33}$$

This is a familiar result.

The boundaries between the four regimes described above are sketched in Fig. 1.

IV. NUMERICAL RESULTS

To evaluate the matching parameter $\Delta(\omega)$ numerically we make use of the fact that Fourier transformation of the equations (8)-(9) reduces the order of the problem from six to two. Before extracting the matching parameter from the solution of the Fourier transformed problem, however, we must address the fact that the layer solution exhibits a secular divergence at large distances from the resonant surface, so that the Fourier transform of the solution is ill-defined.

To obtain a well-defined Fourier transform we multiply the equation by the step function $\Theta(x)$ before applying the transform. The transform is then well-defined for $\Im(k) > 0$, and can be defined for real k by a limiting process. This procedure is equivalent to taking a Laplace transform, and leads to the inhomogeneous differential equation

$$\frac{d}{dk}\left[\frac{k^2}{Q - Q_* + ik^2}\frac{d\hat{\Upsilon}}{dk}\right] + \frac{(Q + iPk^2)Qk^2}{Q - Q_* + R^2k^2(Q + iPk^2)}\hat{\Upsilon} = S(k). \tag{34}$$

The inhomogeneous term $S(k)$ in (34) is a rational function of k^2 related to the conditions at the origin $\Xi'(0)$, $\Xi'''(0)$, and $\Psi(0)$. It is analytic in the neighborhood of the origin. The divergence of the original solution at large x manifests itself as a singularity of the Fourier-transformed equation at the origin. Our task is to find the simplest way to calculate the matching parameter $\Delta(Q)$ from the solution of the Fourier transformed equation.

The general solution of Eq. (34) may be expressed as the sum of a particular solution of the inhomogeneous equation and of the general solution of the homogeneous equation. It may easily be seen from the series solution of the inhomogeneous equation near the origin that the equation admits a solution that is regular at the origin (aside from inconsequential logarithmic singularities). This solution must be combined with solutions of the homogeneous equation in order to construct a solution that is well-behaved at large k. The solutions of the homogeneous equation, however, are singular at the origin. It follows that the singular behavior of the Fourier-transformed solution at small k is entirely determined by the solutions of the homogeneous equation, and that the matching parameter may be determined by matching the solutions of the homogeneous equation to the small-k expansion

$$\hat{\Xi}(k) \sim \frac{\Delta(Q)}{\pi k} + 1 + O(k) \tag{35}$$

The numerical procedure is then straightforward. The solution is initialized at large k with an asymptotic solution of the homogenous form of Eq. (34). It is then integrated

inwards until it matches the form given by Eq. (35). The starting and end points for the integration are adjusted based on analytical estimates of the mode width and current channel width. The island response parameter $\hat{\Delta}(Q)$ is then extracted by taking the ratio of the Wronskians of the solution with the small ($\Xi \sim 1$) and large ($\Xi \sim 1/k$) solutions of the homogeneous equation found through a Fuchs series expansion.

In order to interpret the force curves, we briefly review the theory of mode penetration. Recall that the equilibrium plasma rotation is found by balancing the electromagnetic force given in Eq. (7) with the viscous force resulting from the tendency of the resonant layer to be entrained by the bulk plasma motion. The equilibrium frequency is thus found to be given by the intersection between the graph of the electromagnetic force and that of the viscous force. The graph of the electromagnetic force can be made universal by normalizing the force to the square of the vacuum perturbation amplitude (the force thus normalized is simply $\Im(1/\Delta(Q))$. The viscous force is proportional to the difference between the actual rotation frequency Q at the resonant layer and the rotation frequency Q_0 that would be found in the absence of perturbation, termed the "natural" rotation frequency. It is thus represented by a straight line going through the point $(Q_0, 0)$ and with a slope inversely proportional to the square of the vacuum field perturbation (Fig. 5).

Mode penetration can be seen to result when the slope of the viscous force line decreases until its intersection with the electromagnetic force curve disappears at the point where the two curves are tangent. At that point, marked A in Fig. 5, the rotation makes a rapid transition to the only remaining intersection point between the electromagnetic and viscous force curves, marked B. Due to the steepness of the electromagnetic force curve at the resonant frequencies $\omega = 0$ and $\omega = \omega_{*e}$ (see Figs. 2 and 3), the resulting rotation frequency, characterizing the locked state, is almost indistinguishable from the resonant frequency. Note also that the steepness of the electromagnetic force curve at the resonant frequencies implies that a root to the force balance equation exists for all values of the viscous force up to the critical penetration force.

The normalized electromagnetic force curve for $R = 4$, $Q_* = 1$, and $P = 5$ is compared in Fig. 5 to that for the short mean-free-path case $R = Q_* = 0$. We see that the main difference between the two curves is due to the emergence of a resonance at $Q = Q_*$ in the drift-MHD calculation. The long mean-free-path corrections are typically a factor of two or less for the moderate values of R encountered in fusion experiments. These moderate values

of R also account for the poor fit between the analytic and numerical result for the *phase* of the perturbation at low frequency, as can be seen in Fig. 4. Fortunately the analytic result for the *force* is in much better agreement with the numerical result, even for moderate R.

The presence of two roots where the electromagnetic force is resonant suggests that low-density locked modes (LDLMs) could appear at two different plasma rotation frequencies depending on the direction of the natural plasma rotation. We note however, that stability requires that

$$F'_{\rm EM}(Q) > F'_{\rm V}(Q),$$

where the primes denote derivation with respect to Q. When this stability condition is violated, a small acceleration (caused by turbulence-driven zonal flows for example) will lead to a continuous acceleration of the plasma away from the equilibrium solution. Inspection of the roots near $Q = 0$ shows that only one of the two branches satisfies the stability condition, but since the two roots are extremely close together (Fig. 3), the entire $Q \ll 1$ region may be considered unstable. We conclude thus that the final rotation after mode penetration will be $Q \simeq Q_*$: that is, after mode penetration, the plasma velocity will adjust so that the electric drift balances the diamagnetic drift, leaving the electrons at rest in the frame of the perturbation.

The scaling of the force and penetration threshold with machine size is of interest in the context of the burning plasma experiment being planned. We have examined the scaling using the model of Fitzpatrick for Ohmic discharges.[17] We find that of the three dimensionless parameters governing the resonant force, only P varies significantly with the size of the plasma. Surprisingly, the penetration threshold turns out to have virtually the same scaling with plasma size as predicted by the MHD model. It follows that long mean-free-path effects do not modify the previously calculated symmetry requirements for burning plasma devices.

V. DISCUSSION

We have shown that magnetic perturbations exert a force near resonant surfaces that is such as to bring the electrons to rest in the frame of the perturbation. It follows that in an axisymmetric device where poloidal rotation is damped, static perturbations (error fields) will induce plasma rotation in the direction of the electric current (co-rotation). Since

the electromagnetic force imposed by the perturbation is highly localized, one infers that significant local modifications to the rotation profile may result from the brief application of small resonant fields. This could be achieved with the use of internal coils, such as those presently being installed on the DIII-D tokamak.[38]

Our results also suggest that for finite ion temperature, a new root with vanishing force is likely to appear at the ion diamagnetic frequency. The direction of the force in this case is unclear but is likely to depend on the plasma velocity. This will be the subject of a future investigation.

Lastly, we have shown that long mean free path effects have a quantitatively modest effect on the force and penetration threshold for parameters typical of fusion plasmas. This is due to the approximate compensation between the effect of decreasing $\rho_* = \rho_i/L$, the ratio of the gyroradius to the system size, and the effect of increasing the Lundquist number $S = \delta^{-3}$.

Acknowledgment This work is funded by the US DoE contract number DE-FG03-96ER-54346.

Appendix A: Matching of the inner and outer layers:

In this appendix we extend the analysis of section III to include the effect of the resonant-surface flux $\Psi(0)$. This makes it possible to demonstrate the smooth matching of the solutions in the current channel and the vorticity (outer) layer. In order to do this we begin by solving Eq. (19) for the response to the inductive field at the resonant surface. To solve this equation, we eliminate the inhomogeneous term by multiplying by X and taking the derivative. We then look for solutions of the resulting equation in the form

$$\Xi(X) = \int_{p_1}^{p_2} dp\, e^{-pX} \hat{\Xi}(p). \tag{A.1}$$

where the integration bounds p_1 and p_2 are specified later. This leads to

$$\int_{p_1}^{p_2} dp\, p e^{-pX} \frac{d}{dp}[M(p)\Xi(p)] - \left[p e^{-pX} M(p) \hat{\Xi}(p) \right]_{p_1}^{p_2} = 0 \tag{A.2}$$

where the quantity in brackets represents boundary terms left over after integration by parts. The integral vanishes for

$$\hat{\Xi} = \Xi_0 / E(p), \tag{A.3}$$

where Ξ_0 is an integration constant that will be determined later so as to satisfy Eq. (19). The boundary term in Eq. (A.1) reduces then to $[\Xi_0 p e^{-pX}]_{p_1}^{p_2}$. This can be made to vanish by choosing $p_1 = 0$, $p_2 = \infty$. Carrying out the integral in Eq. (A.1) with the solution in Eq. (A.3), we then find

$$\Xi(x) = \frac{(Q - Q_*)\Psi(0)}{2R^2 P(\lambda_+^2 - \lambda_-^2)} \left[\frac{\mathcal{E}(\lambda_+ x)}{\lambda_+} - \frac{\mathcal{E}(\lambda_- x)}{\lambda_-} \right] \tag{A.4}$$

where

$$\mathcal{E}(z) = e^z E_1(z) - e^{-z} Ei(z) \tag{A.5}$$

and where we have calculated the constant Ξ_0 so as to satisfy Eq. (19).

It is now a simple matter to match the inner and outer solutions. Substituting the solution for the outer layer given by Eqs. (A.4)-(A.5) into Eq. (23) and using the small argument expansion of $\mathcal{E}$,

$$\mathcal{E}(z) \sim -2(\gamma + \ln z) + O(z \ln z),$$

where γ is Euler's constant, we find

$$\Gamma(X) = \Gamma_\infty - \frac{Q(Q - Q_*)\Psi(0)}{R^2} \left(\gamma + \frac{\lambda_+^2 \ln \lambda_+ + \lambda_-^2 \ln \lambda_-}{\lambda_+^2 - \lambda_-^2} + \ln X \right) \tag{A.6}$$

We next integrate Ohm's law over the inner, current channel region to find

$$\Gamma(X) = -\Psi(0) - \frac{Q(Q - Q_*)\Psi(0)}{2R^2} \ln(1 + iX^2 R^2/Q) \tag{A.7}$$

The logarithmic singularity of the inner and outer solutions clearly match. Eliminating $\Gamma(X)$ between these two equations leads to a corrected formula for the layer response parameter $\hat{\Delta}(Q)$:

$$\frac{1}{\hat{\Delta}(Q)} = \frac{1}{\Delta_{\text{out}}} + \frac{1}{\Delta_{\text{ch}}} \left[1 + \frac{Q(Q - Q_*)}{2R^2} \left(\gamma + \frac{\lambda_+^2 \ln \lambda_+ + \lambda_-^2 \ln \lambda_-}{\lambda_+^2 - \lambda_-^2} - \ln \frac{R^2}{Q} \right) \right] \tag{A.8}$$

The correction can be seen to be small in all regimes of interest.

[1] A. M. Garofalo, T. H. Jensen, L. C. Johnson, R. J. L. Haye, G. A. Navratil, M. Okabayashi, J. T. Scoville, E. J. Strait, D. R. Baker, J. Bialek, M. S. Chu, J. R. Ferron, J. Jayakumar, L. L. Lao, M. A. Makowski, H. Reimerdes, T. S. Taylor, A. D. Turnbull, M. R. Wade, and S. K. Wong, Phys. Plasmas **9**, 1997 (2002).

[2] A. M. Garofalo, A. D. Turnbull, M. E. Austin, J. Bialek, M. S. Chu, K. J. Comer, E. D. Fredrickson, R. J. Groebner, R. J. L. Haye, L. L. Lao, E. A. Lazarus6, G. A. Navratil, T. H. Osborne, B. W. Rice, S. A. Sabbagh, J. T. Scoville, E. J. Strait, and T. S. Taylor, Phys. Rev. Lett. **82**, 3811 (1999).

[3] A. Garofalo, R. L. Haye, and J. Scoville, Nucl. Fusion **42**, 1335 (2002).

[4] J. M. Finn, Phys. Plasmas **2**, 198 (1995).

[5] M. Persson, R. L. Dewar, and E. K. Maschke, Phys. Fluids B **5**, 3844 (1993).

[6] C. Hegna, Phys Plasma **6**, 130 (1999).

[7] A. W. Morris, Phys. Rev. Lett. **64**, 1254 (1990).

[8] R.Fitzpatrick, Phys. Plasmas **4**, 2519 (1997).

[9] R. Fitzpatrick and T. Jensen, Physics of Plasmas **3**, 2641 (1996).

[10] R. Fitzpatrick and T. C. Hender, Phys. Fluids B **3**, 644 (1991).

[11] R. J. L. Haye, R. Fitzpatrick, T. C. Hender, A. W. Morris, J. T. Scoville, and T. N. Todd, Phys. Fluids B **4**, 2098 (1992).

[12] A. H. R.J. La Haye and J. Scoville, Nucl. Fusion **32**, 2119 (1992).

[13] A. W. Morris, P. G. Carolan, R. Fitzpatrick, T. C. Hender, and T. N. Todd, Phys. Fluids B **4**, 413 (1992).

[14] R. D. Parker, Proceedings of the 19th EPS-ICPP conf., Innsbruck, 1992, edited by K. Bethge (European Physical Society, Geneva, 1993), **1**, 427 (1992).

[15] A. H. Reiman and D. A. Monticello, Nucl. Fusion **32**, 1341 (1992).

[16] T. H. Jensen, A. W. Leonard, and A. W. Hyatt, Phys. Fluids B **5**, 1239 (1993).

[17] R. Fitzpatrick, Nuclear Fusion **33**, 1049 (1993).

[18] G. M. Fishpool and P. S. Haynes, Nucl. Fusion **34**, 109 (1994).

[19] R. Fitzpatrick and T. C. Hender, Phys. Plasmas **1**, 3337 (1994).

[20] O. A. Hurricane, T. H. Jensen, and A. B. Hassam, Phys. Plasmas **2**, 1976 (1995).

[21] A. Boozer, Phys. Plasmas **3**, 4620 (1996).

[22] T. H. Jensen, R. J. L. Haye, and A. W. Hyatt, Phys. Plasmas **3**, 1524 (1996).

[23] A. Boozer, Phys. Rev. Lett. **86**, 5059 (2001).

[24] J. Cary and M. Kotschenreuther, Phys Fluids **28**, 1392 (1984).

[25] T. C. Hender, R. Fitzpatrick, A. W. Morris, P. G. Carolan, R. D. Durst, T. Edlington, J. Ferreira, S. J. Fielding, P. S. Haynes, J. Hugill, I. J. Jenkins, R. J. L. Haye, B. J. Parham, D. C. Robinson, T. N. Todd, M. Valovic, and G. Vayakis, Nucl. Fusion **32**, 2091 (1992).

[26] R. J. L. Haye and O. Sauter, Nucl. Fusion **38**, 987 (1998).

[27] R. Fitzpatrick and F. L. Waelbroeck, Phys. Plasmas **7**, 1 (2000).

[28] J. F. Drake and Y. C. Lee, Phys Fluids **20**, 1341 (1976).

[29] J. F. Drake, Phys Fluids **21**, 1777 (1978).

[30] S. M. Mahajan, R. D. Hazeltine, H. R. Strauss, and D. W. Ross, Phys. Fluids **22**, 2147 (1979).

[31] R. D. Hazeltine and J. D. Meiss, Phys. Reports **121**, 1 (1985).

[32] D. Biskamp, Nucl. Fusion **18**, 1059 (1978).

[33] J. F. Drake, T. M. Antonsen, A. B. Hassam, and N. T. Gladd, Phys Fluids **26**, 2509 (1983).

[34] H. P. Furth, P. H. Rutherford, and H. Selberg, Phys. Fluids **16**, 1054 (1973).

[35] B. Coppi, R. Galvao, M. N. Rosenbluth, P. H. Rutherford, and R. Pelat, Sov. J. Plasma Phys. **2**, 1894 (1976).

[36] G. Ara, A. Basu, and B. Coppi, Ann. Phys. **112**, 443 (1978).

[37] R. Fitzpatrick, Phys. Plasmas **1**, 3308 (1994).

[38] J. L. Luxon, Nucl. Fusion **42**, 614 (2002).

LIST OF FIGURES

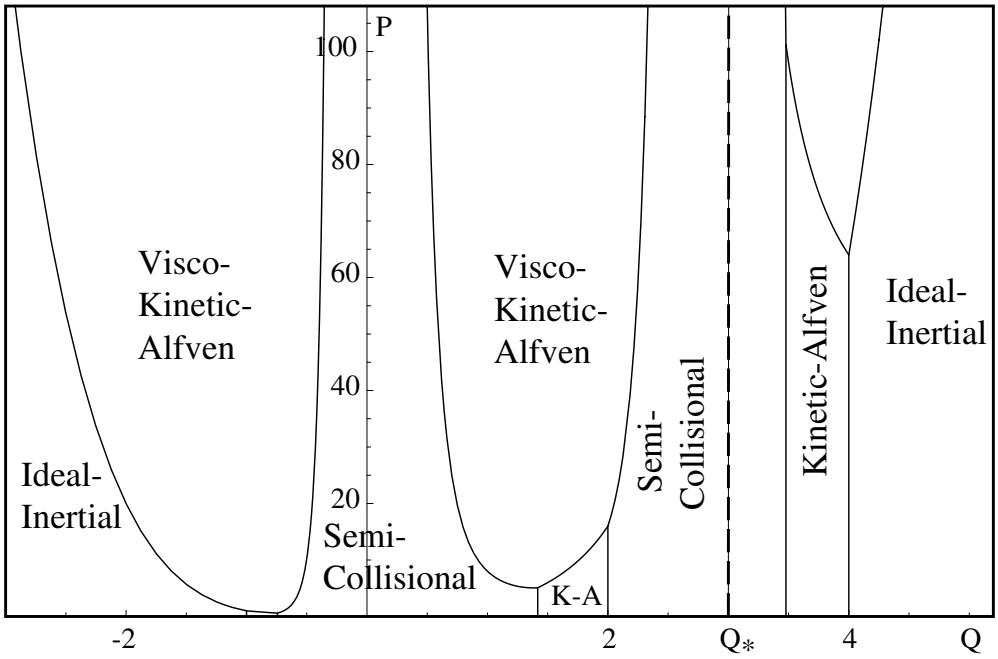
P
100
80
60
40
20
Visco-
Kinetic-
Alfven
Ideal-
Inertial
Semi-
Collisional
Visco-
Kinetic-
Alfven
K-A
Semi-
Collisional
Kinetic-Alfven
Ideal-
Inertial
-2
2
Q*
4
Q

FIG. 1:

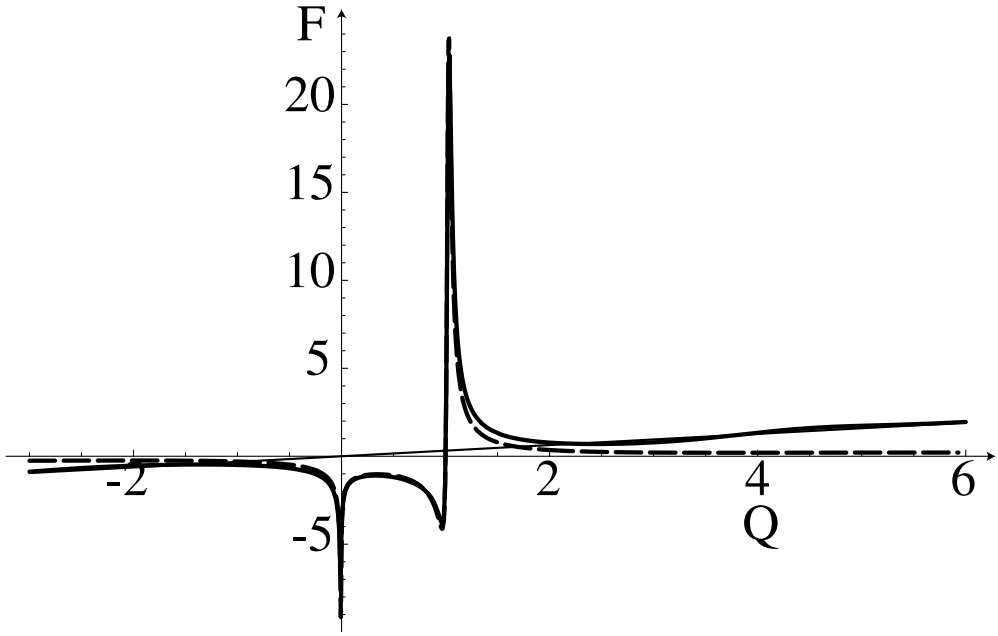
F
20
15
10
5
-5
-2
2
4
6
Q

FIG. 2:

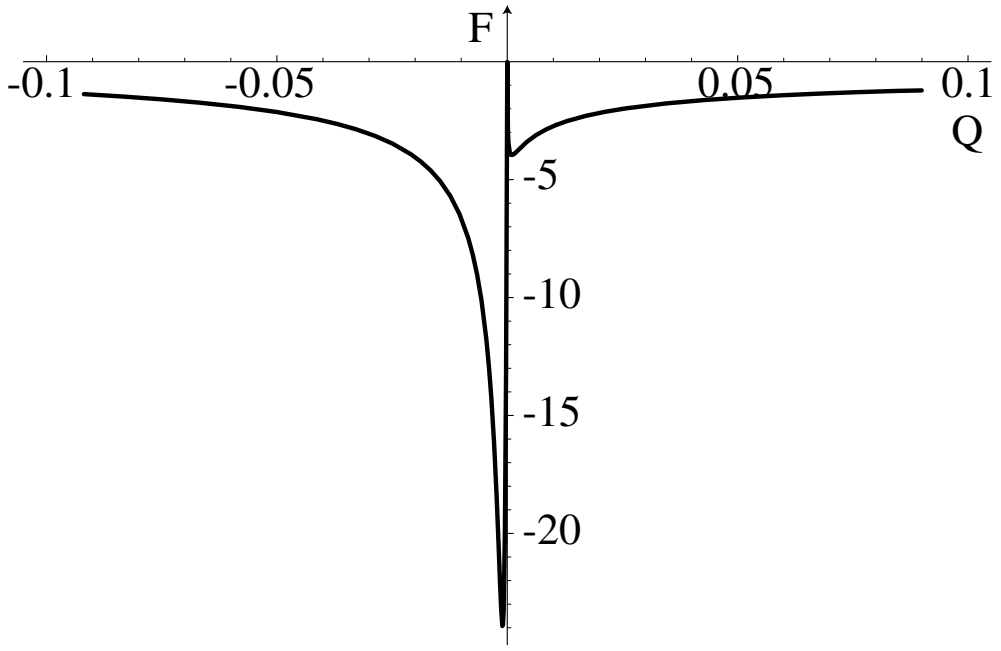

FIG. 3:

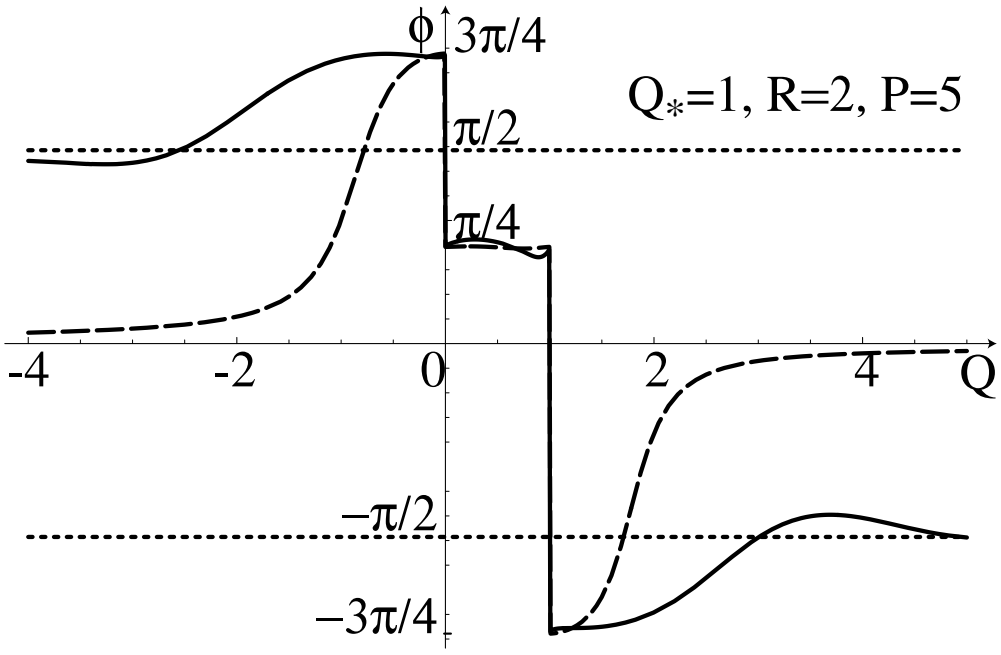

FIG. 4:

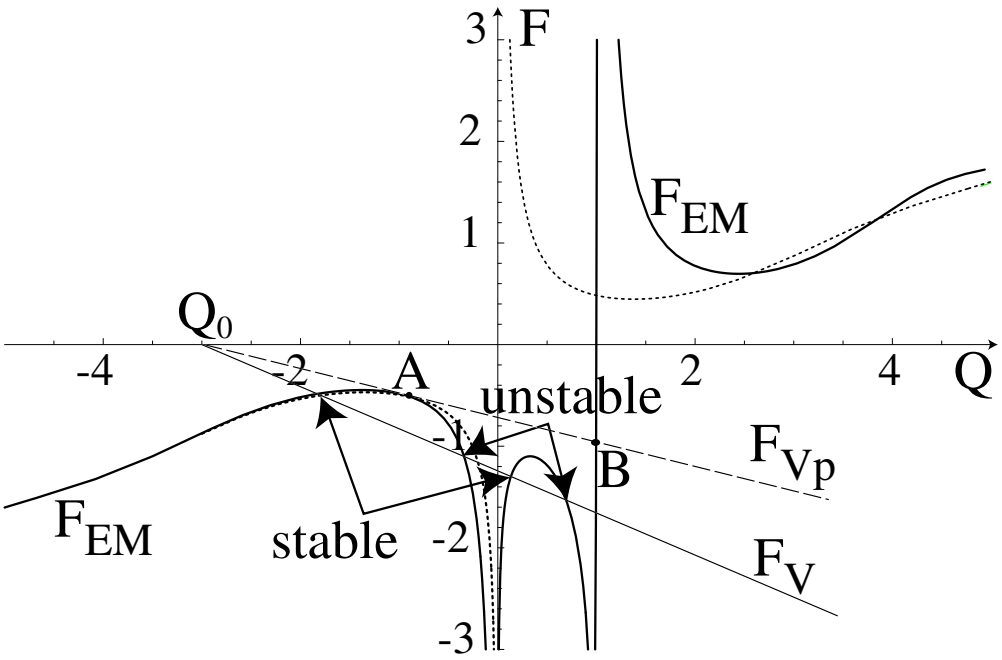
F
3
2
1
-1
-2
-3
-4
-2
A
2
4
Q
Q_0
F_{EM}
unstable
B
F_{Vp}
F_V
stable
F_{EM}

FIG. 5:

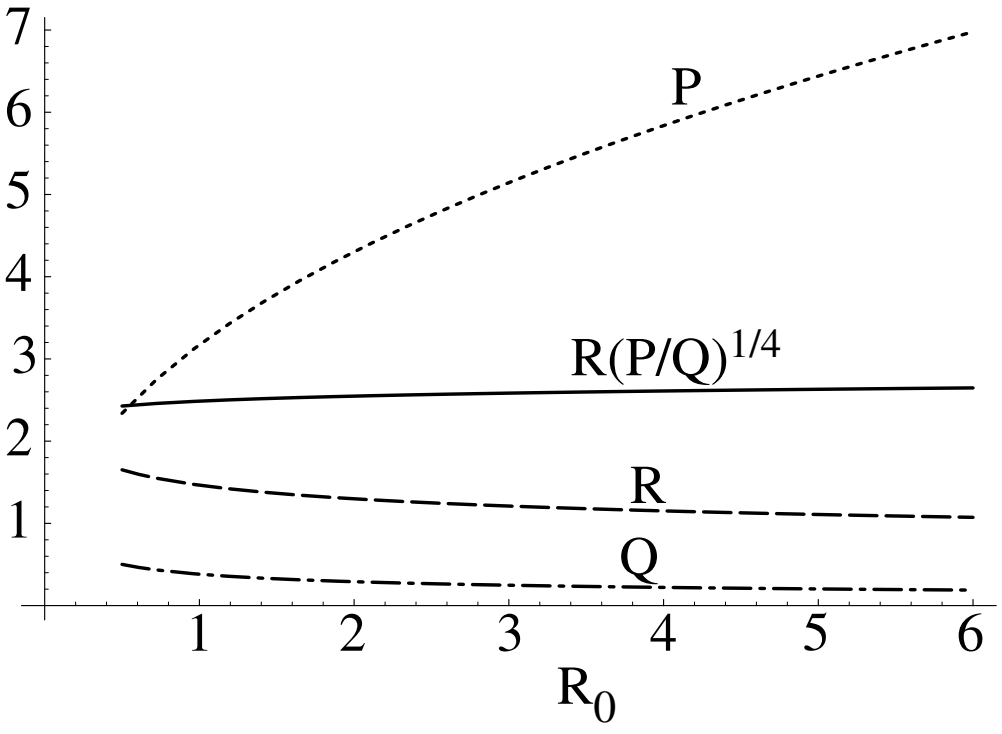
7
6
5
4
3
2
1
P
$R(P/Q)^{1/4}$
R
Q
1
2
3
4
5
6
R_0

FIG. 6:

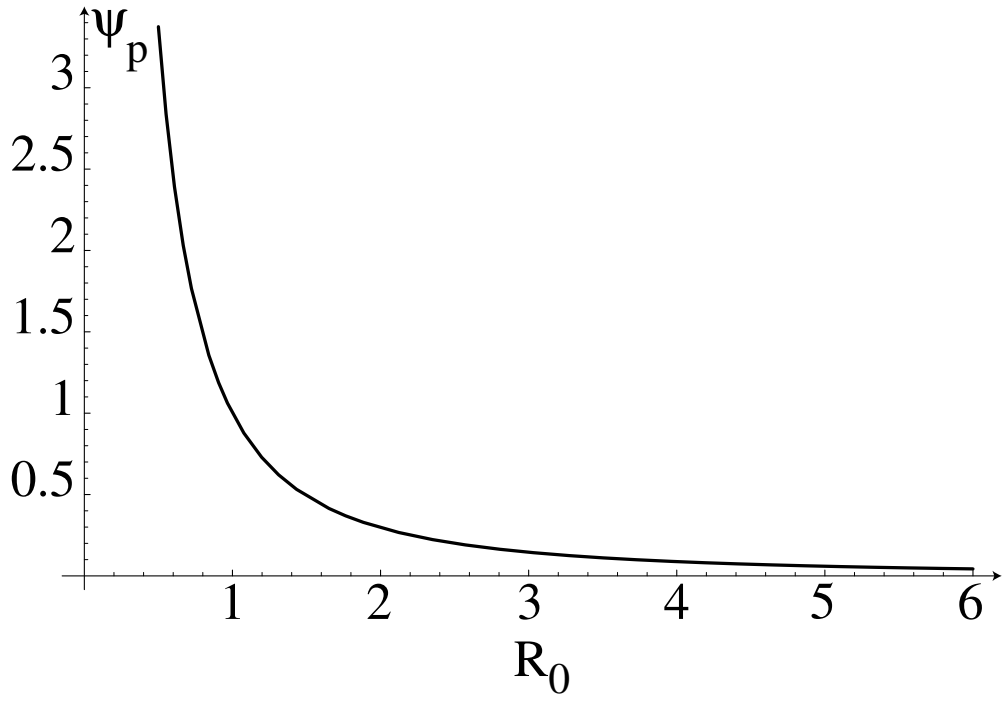

FIG. 7: